International Journal of Thermofluid Science and Technology (2023)
Volume 10, Issue 4, Paper No. 100402
https://doi.org/10.36963/IJTST.2023100402

Research Article

# Natural convection of power-law fluid in a horizontal annulus between outer cylinder and inner flat tube

Benhizia Oussama[*, 1], Bouzit Mohamed[2]

[1] *Department of Mechanical Engineering, Faculty of Applied Sciences, University of Kasdi Merbah Ouargla, Route de Ghardaia, BP.511, 30000 Ouargla, Algeria*
[2] *Faculty of Mechanical Engineering, Department of Mechanics, University of Sciences and Technology of Oran Mohamed Boudiaf, BP. 1505 Oran El M'Naouer, 31000, Oran, Algeria*

ATICLE INFO

Received: 01 Aug. 2023;
Received in revised form:
28 Oct. 2023;
Accepted: 07 Nov. 2023;
Published online:
22 Nov. 2023

*Keywords:*
Natural convection
Non-Newtonian fluid
Power-law model
Horizontal flat tube
Nusselt number

## ABSTRACT

Natural convection in two-dimensional space created by putting horizontal flat tube concentrically in cooled horizontal cylinder is studied numerically. The model solved using the ANSYS CFX package. The numerical simulations covered a range of power-law index $0.6 \leq n \leq 1.4$, Prandtl number $10 \leq Pr \leq 10^3$ and Rayleigh number $10^3 \leq Ra \leq 10^5$. The effects of the previous parameters on the flow pattern, the average Nusselt number and the dimensionless temperature and velocity profiles have been investigated.

The results showed that the average Nusselt number increases with increasing Rayleigh number and decreases with increasing the power-law index. The best case among the range of parameters considered here is the heat transfer rate of pseudo-plastic fluids (n=0.6), then the Newtonian fluids (n=1) and finally, the dilatant fluids (n=1.4). It is shown that the sharpness cooling effect of pseudo-plastic fluids and the sharpness insulating effect of dilatant fluids hugely affected by the increasing of Rayleigh number. The Prandtl number has almost no effects on the heat transfer rate in the range considered here. The results for the average Nusselt number and the dimensionless temperature have been compared versus some previous works and showed good agreement.



## 1. Introduction

Heat transfer enhancement is one of the major engineering applications. It caught a considerable attention in the last recent years because of its large uses like solar collectors, cooling of electronic equipment, nuclear reactors and heat exchangers where the heat transfer from tubes of elliptic shapes was the subject of many researchers in the last few years because they found to lessen the resistance to the cooling fluid.

The entropy generation due to natural and mixed convection heat transfer was introduced by [1-5]. The authors found out that the local and average heat transfer rates and the entropy generation increase with increasing the nanoparticles volume fraction and the porous medium permeability.

[*]*Corresponding e-mail*: benhizia_oussama@yahoo.fr

**Nomenclature**

| | | | |
|---|---|---|---|
| $C_p$ | Specific heat capacity, J kg$^{-1}$K$^{-1}$ | $u_i$ | $i$th velocity component, m s$^{-1}$ |
| $e_{ij}$ | Rate of strain tensor, s$^{-1}$ | $u,v$ | Radial and tangential velocities, m s$^{-1}$ |
| $g$ | Gravity acceleration, m s$^{-2}$ | $\bar{u},\bar{v}$ | Dimensionless radial and tangential velocities |
| $h$ | Heat transfer coefficient, W m$^{-2}$ K$^{-1}$ | $x,y$ | Cartesian coordinates |
| $k$ | Thermal conductivity, W m$^{-1}$ K$^{-1}$ | $X,Y$ | Dimensionless cartesian coordinates |
| | | $x_i$ | Coordinate in the $i$th direction, m |
| $K$ | Consistency index of the power-law | *Greek symbols* | |
| $L$ | Characteristic Length, m | $\alpha$ | Thermal diffusivity, m$^2$ s$^{-1}$ |
| $n$ | Power-law index | $\beta$ | Volume coefficient of expansion, K$^{-1}$ |
| $Nu_{ave}$ | Average Nusselt number $\frac{h\,L}{k}$ | $\tau_{ij}$ | Stress tensor, Pa |
| $P$ | Pressure | $\Delta T$ | Difference between hot and cold temperatures, $T_h$–$T_c$ |
| $Pr$ | Prandtl number $\frac{\mu\, C_p}{k}$ | $\theta$ | Dimensionless temperature |
| $Ra$ | Rayleigh number $\frac{\rho^2 g\beta C_p \Delta T L^3}{\mu\, k^2}$ | $\mu$ | Dynamic viscosity, N s m$^{-2}$ |
| $R$ | Radius, m | $\mu_a$ | Apparent viscosity |
| $\overline{R}$ | Dimensionless Radius | $\rho$ | Density, Kg m$^{-3}$ |
| $T$ | Temperature | $\rho_0$ | Reference density |
| $T_h$ | Inner flat tube temperature, °K | $\phi$ | Orientation angle, ° |
| $T_c$ | Outer cylinder temperature, °K | | |

The problem of double-diffusive binary gas mixture convective flow in rectangular and inclined rectangular enclosures was studied by Chamkha [6], Chamkha and Al-Naser [7] respectively. The maps of temperature contours, streamlines and the concentrations are presented. Also, the effects of the buoyancy ratio on the average Nusselt and Sherwood numbers are discussed.

Ismael et al. [8] and Umavathi et al [9] studied the effects of viscous and darcy dissipations on mixed convection. Chamkha et al. [10] studied the mixed convection of air inside a square vented cavity. They found out that the viscous dissipation enhances the flow in the downward case where it counters the flow in the upward case. Moreover, they developed an empirical correlation by using the Nusselt, Reynolds and Richardson numbers.

Hussain and Hussein [11] conducted a numerical study on the natural convection heat transfer of moving heated circular cylinder in square enclosure in the first time and Hussein [12] in parallelogrammic cavity in the other time. Saha et al. [13] took the problem from another side and studied the effects of the diameter ratio of the adiabatic cylinder and the inclination angle of the opened enclosure on the heat transfer characteristics. Li et al. [14, 15] added the thermal radiation effects on natural convection of nanofluid in an inclined square cavity.

Sakr et al. [16] conducted experimental and numerical studies on the free convection heat transfer in a gap between inner elliptic cylinder and outer one, the effects of Rayleigh number, hydraulic radius ratio and orientation angle of the inner cylinder on the heat transfer were widely discussed. Alawi et al. [17] developed the same problem numerically in a horizontal gap formed by constant heat flux flat tube concentrically located in cooled cylinder but using $SiO_2$ nanofluid.

The study of non-Newtonian power-law fluids over bodies of different geometries has caught a great attention in the past few years

because of their uses in applications such as compact heat exchangers, food processing, chemical processing, solar collector systems and polymer engineering. Therefore, [18-21] proved that the power law index n and the Rayleigh number affect the drag coefficient and the Nusselt number in which the increase in the shear thinning tendency enhances the rate of heat transfer by up to three folds and decreases the apparent viscosity and impede it about 30–40% in the shear thickening fluids.

Hussain et al. [22], Hussein et al. [23] Analysed the free convection heat transfer in tilted sinusoidal corrugated enclosure in the presence of longitudinal magnetic field, they set a new correlation for the Nusselt number as a function of the different parameters and revealed a new way to enhance the heat transfer by decreasing the surface length. Uddin et al. [24] conducted a 2D numerical study of the convective heat transport of nanofluid filled in vertical tube of plain and corrugate side walls, they proved that the heat transfer rate for the tube of corrugate side walls is higher at low thermal Rayleigh numbers.

The power-law fluids were used in studies such as electroosmotic and pressure driven flows [25] for finding a new correlation for the average Nusselt number [26]. Hence, the steady states laminar natural convection [27-31], Rayleigh-Bénard configuration [32] in a cavity where it was heated from below and in the case of differentially heated vertical walls were studied numerically. The authors used the power law model to simulate the non-Newtonian fluid and the difference of temperature between the horizontal walls can produce buoyancy driven flow. It was found that the average Nusselt number in the differentially heated horizontal walls is smaller than that of the differentially heated side walls (vertical walls case).

Hussein et al. [33] analysed the 3D unsteady natural convection case of cubical trapezoidal cavity that takes longer time and adequate conditions in the simulation for the solution to converge, Alnaqi [34] developed the same problem but considering active lateral walls.

Gourari et al. [35] determined the heat transfer rate in the gap between two concentric inclined cylinders at 0°, 45° and 90°, they proved that the heat transfer is the highest at 90°. Elkhazen et al. [36] studied the electroconvection of dielectric fluid between two confocal elliptical cylinders in the polar coordinates, they coupled the Navier Stokes and the Maxwell equations in their model to solve the governing equations.

Mixed convection heat transfer of nanofluids has been studied numerically in different body shapes like square enclosure, circular enclosure and inclined baffled C-shaped enclosure [37-39]. The authors include the effects of the different parameters on the heat transfer characteristics in their analysis. Bougoul et al. [40] used nanofluids to optimize the thermal efficiency of a reduced air solar collector, they presented the flow structure and the different heat transmission mechanisms in the gap.

The effect of inserting an adiabatic solid strip/square enclosure as blocks in the center of the cavity of triangular roof/square cavity on natural convection has been done numerically by Hussein et al. [41, 42], the authors gave detailed explanations of its impacts on the thermal performance. Islam et al. [43], Akhter et al. [44] developed the issue of natural convection of nanofluid in a right-angled triangular cavity and in an enclosure of heated hexagonal block, respectively. Ghoben and Hussein [45] went further in their analysis and make it in 3D triangular cavity of heated cylindrical tube with different arrangements. Ashraf et al. [46] studied the bioconvection of nanofluid of irregular thickness across a slender elastic surface, the velocity and temperature profiles are drawn and discussed.

Baïri et al. [47] were the first to propose a correlation between the Nusselt and Rayleigh numbers for a closed gap between concentric semi-hemispheres. This correlation is valid for electronic packaging, buildings and architecture. Kar et al. [48] analysed the heat transfer enhancement in square enclosure heated at the bottom and cooled at the top using four parallel vertical partitions. Kim et al. [49] studied the geometrical effect on the thermal behavior and

heat removal performance in a channel with a cavity at the turning section. Dong et al. [50] investigated numerically the natural convection in the passive containment air-cooling system where the dome is an essential part from it, the different effects of natural convection around the dome were presented and discussed.

According to the previous literature, too many studies were performed on the natural convection between two cylinders but few of them treated the problem when the inner cylinder is elliptic or flat plate in case the axis ratio is so small. In this study, we involved the non-Newtonian power law fluids as working fluid which is a kind of expansion in the study of this type of geometries. An effort has been made to explore the effects of the different parameters on the flow patterns and the heat transfer in the numerical domain.

## 2. Description of the problem

The schema of the physical and numerical domains is shown in Fig. 1. An annulus is filled with non-Newtonian power law fluid. The problem is that the inner horizontal flat tube heated isothermally at temperature $T_h$ while the outer cylinder is cooled under temperature $T_c$ ($T_h$>$T_c$). Due to the small temperature difference between the flat tube and the outer cylinder a buoyancy induced flow takes place within the power law and the Boussinesq assumption is applied on the density forces. The changes of density with the temperature T may be written as

$$\rho= \rho_0 (1-\beta(T-T_i))$$

It is worth mentioning that the angle which corresponds to $\phi$=0° is toward the bottom of the outer cylinder (the same direction as the gravity force is). The velocity and temperature fields in the flow domain are governed by equations of continuity, momentum and thermal energy as following

$$\frac{\partial u}{\partial x}+\frac{\partial v}{\partial y}=0 \quad (1)$$

$$\rho u\frac{\partial u}{\partial x}+\rho v\frac{\partial u}{\partial y}=-\frac{\partial P}{\partial x}+\mu\left(\frac{\partial^2 u}{\partial x^2}+\frac{\partial^2 u}{\partial y^2}\right) \quad (2)$$

$$\rho u\frac{\partial v}{\partial x}+\rho v\frac{\partial v}{\partial y}=-\frac{\partial P}{\partial y}+\mu\left(\frac{\partial^2 v}{\partial x^2}+\frac{\partial^2 v}{\partial y^2}\right)+\rho g\beta\,(T-T_c) \quad (3)$$

$$\rho C_p u\frac{\partial T}{\partial x}+\rho C_p v\frac{\partial T}{\partial y}=k\left(\frac{\partial^2 T}{\partial x^2}+\frac{\partial^2 T}{\partial y^2}\right) \quad (4)$$

The temperature when the fluid properties are taken is at $T_f=\frac{T_h+T_c}{2}$

The Rayleigh and Prandtl numbers are

$$Ra=\frac{\rho^2 g\beta C_p \Delta T L^3}{\mu_{ref} k^2} \quad , \quad Pr=\frac{\mu_{ref}\, C_p}{k}$$

For viscous non-Newtonian fluid obeys the power law model, the shear stress tensor can be written as

$$\tau_{ij}=\mu_a e_{ij}=\mathrm{K}\,(e_{kl}e_{kl}/2)^{(n-1)/2}e_{ij} \quad (5)$$

Where $e_{ij}=(\partial u_i/\partial x_j+\partial u_j/\partial x_i)$ is the shear rate, K is the consistency index and n is the power law index and of course the apparent viscosity is $\mu_a= K\,(e_{kl}e_{kl}/2)^{(n-1)/2}$ (6)

With this form of viscosity, it's clear that $\mu_a$ decreases/increases with increasing the strain tensor rate for n<1/n>1 respectively, and thus two types of fluids are considered here represent shear thinning fluids with n<1 and shear thickening fluids with n>1. These fluids don't obey the rule of Newtonian fluids (the shear stress is not proportional to the shear strain and doesn't have a linear relation with it) and they're particular with their apparent viscosity $\mu_a$ in which it decreases with increasing shear rate (case of pseudo-plastic fluids) and increases with decreasing the shear rate (case of dilatant fluids). The apparent viscosity for a power law fluid in the Cartesian coordinate is

$$\mu_a=\mathrm{K}\left[2\left(\left(\frac{\partial u}{\partial x}\right)^2+\left(\frac{\partial v}{\partial y}\right)^2\right)+\left(\frac{\partial v}{\partial x}+\frac{\partial u}{\partial y}\right)^2\right]^{\frac{n-1}{2}} \quad (7)$$

The Rayleigh and Prandtl numbers after we introduced $\mu_a$ becoming

$$Ra=\frac{\rho g\beta\Delta T L^{2n+1}}{\alpha^n K} \quad , \quad Pr=\frac{KL^{2-2n}}{\rho\alpha^{2-n}} \quad (8)$$

The local and average Nusselt numbers are

$$Nu_L=-\frac{\partial\theta}{\partial\bar{R}} \quad , \quad Nu_{ave}=\frac{1}{2\pi}\int_0^{2\pi} Nu_L\,d\phi \quad (9)$$

The dimensionless quantities are assigned as follow

$$\mathrm{P}=\frac{L^2 p}{\rho\alpha^2} \quad , \quad \theta=\frac{T-T_c}{T_h-T_c} \quad , \quad \bar{u}=\frac{\mathrm{L}u}{\alpha} \quad , \quad \bar{v}=\frac{\mathrm{L}v}{\alpha}$$

$$\bar{R}=\frac{\mathrm{R}}{L} \quad , \quad \mathrm{X}=\frac{x}{R} \quad , \quad \mathrm{Y}=\frac{y}{R}$$

The previous governing equations in the dimensionless form become

$$\frac{\partial \bar{u}}{\partial X} + \frac{\partial \bar{v}}{\partial Y} = 0 \quad (10)$$

$$\bar{u}\frac{\partial \bar{u}}{\partial X} + \bar{v}\frac{\partial \bar{u}}{\partial Y} = -\frac{\partial P}{\partial X} + \Pr\left[2\frac{\partial}{\partial X}\left(\frac{\mu_a}{K}\frac{\partial \bar{u}}{\partial X}\right) + \frac{\partial}{\partial Y}\left(\frac{\mu_a}{K}\left(\frac{\partial \bar{u}}{\partial Y} + \frac{\partial \bar{v}}{\partial X}\right)\right)\right] \quad (11)$$

$$\bar{u}\frac{\partial \bar{v}}{\partial X} + \bar{v}\frac{\partial \bar{v}}{\partial Y} = -\frac{\partial P}{\partial Y} + \mathrm{Ra}\,\Pr\,\theta + \Pr\left[\frac{\partial}{\partial X}\left(\frac{\mu_a}{K}\left(\frac{\partial \bar{u}}{\partial Y} + \frac{\partial \bar{v}}{\partial X}\right)\right) + 2\frac{\partial}{\partial Y}\left(\frac{\mu_a}{K}\frac{\partial \bar{v}}{\partial Y}\right)\right] \quad (12)$$

$$\bar{u}\frac{\partial \theta}{\partial X} + \bar{v}\frac{\partial \theta}{\partial Y} = \frac{\partial^2 \theta}{\partial X^2} + \frac{\partial^2 \theta}{\partial Y^2} \quad (13)$$

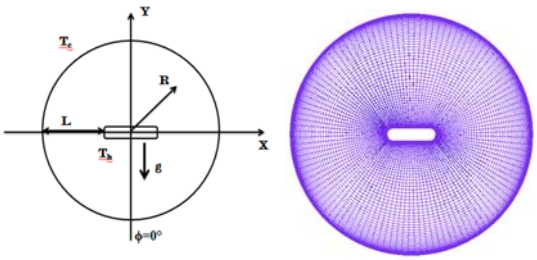


Fig. 1 Physical (left) and Numerical (right) Domains of the Problem.

## 3. Numerical analysis and problem

In our study, the ANSYS CFX package was used. This package is one of the best simulation software for the engineering applications such as computer aided engineering (CAE), finite element analysis (FEA), computational fluid dynamic (CFD)….. It is used to give qualitative results and provide accurate fluid predictions and results. The Finite Volume Method was used to discritize the governing equations in the computational domain, the explicit scheme is used to obtain the discritized equations, the SIMPLE algorithm [51] is used for coupling the pressure and velocity and the second order upwind discrimination schemes are used, for the convective terms High Resolution Sheme is used.

The laminar model was used for all the simulations for the Rayleigh range considered here. The no slip wall is set for the inner flat tube and the outer cylinder while symmetry boundary condition for the rest, the power-law model was used for the non-Newtonian fluid. It is expected that the solution converge when all the residuals of continuity, momentum and energy are less than $10^{-6}$.

### 3.1 Grid study

In order to choose an optimal Mesh for our study, we conducted a Mesh test for 3 Meshes with different number of elements each, the maillage is formed of quadrilateral elements with different number of nodes in the radial and tangential directions respectively, as follow: Mesh 1 (80*120), Mesh 2 (100*160) and Mesh 3 (120*200), the heat transfer rate is measured for each Mesh and then compared between them to calculate the errors ratio. The grid system is uniform in the angular direction but not uniform in the radial direction, it's thicker near the inner and outer surfaces of the cylinders as the Fig. 1 illustrates, this choice of maillage is due to the fact that strong gradients of temperature and velocity are located near the cylinders.

In Table 1, the present Mesh test is conducted for all types of fluids for n=0.6, n=1 and n=1.4 which complies with the smallest and biggest limits of its variation range in this study whereas a moderate values for Rayleigh and Prandtl numbers are taken as $Ra=10^4$, Pr=100.

From the results presented in table 1, the differences in Nusselt number between Mesh 1/Mesh 2 and Mesh 2/Mesh 3 for pseudoplastic, Newtonian and dilatant fluid were 0.112 ٪ and 0.022 ٪, 0.108 ٪ and 0.017٪, 0.097 ٪ and 0.015 ٪; respectively. It is clearly seen that the results between Mesh 2 and Mesh 3 are so close that the errors are slight thus; the grid size (100*160) is used in the numerical solution.

Table 1 Variations of the average Nusselt number for pseudoplastic, Newtonian and dilatant fluids for different number of elements at Ra=$10^4$ and Pr=100.

| | Mesh 1 | | Mesh 2 | | Mesh 3 |
|---|---|---|---|---|---|
| n | Nu | errors | Nu | errors | Nu |
| 0.6 | 10.138 | 0.112 % | 10.15 | 0.022 % | 10.152 |
| 1 | 5.668 | 0.108 % | 5.675 | 0.017 % | 5.675 |
| 1.4 | 2.962 | 0.097 % | 2.965 | 0.015 % | 2.965 |

## 4. Code validation

In order to perform our simulations, a validation test depends on the measurement of heat transfer rate was carried out for 3 orientation angles of the flat tube under the specific conditions of Sakr et al. [16] ($n$=1, Pr=0.71 and RR=6.4 for different orientation angles) and then we compare the obtained results with theirs, note that the inner tube's flat shape is developed from the elliptic shape which they worked on. The inner elliptic cylinder is allowed to be rotated by an angle ϕ from 0° to 90°, to save time we chose only 3 angles (ϕ=0°, ϕ=45° and ϕ=90°) compared to Sakr et al. [16] who increases each time the inclination by 20°. Fig. 2 presents this comparison and the good concurrence between our results against theirs was extracted.

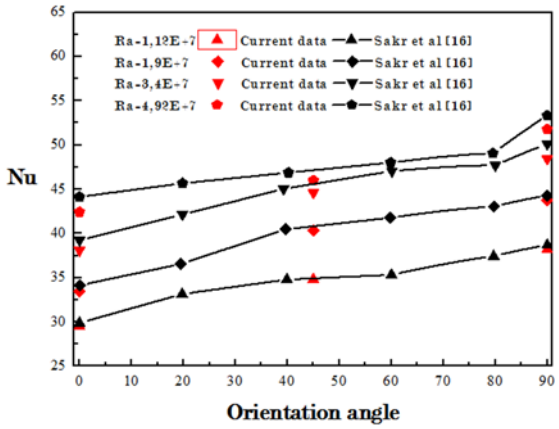


Fig. 2 Comparision between the Nusselt number for the present work and the results of Sakr et al. [16] for n=1, Pr=0.71 RR=6.4 and different Rayleigh numbers.

Moving forward in the procedure, another test was conducted to check the fluid circulation in the gap. This time the benchmark case of Matin & Khan [21] was used to prove the temperature distribution at different angles (ϕ=0°, ϕ=90°, ϕ=180°). The results are illustrated in Fig. 3 and a good agreement between our data and theirs has been detected for all the angles.

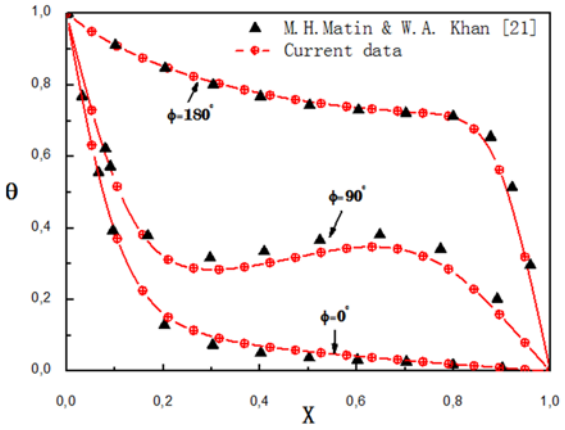


Fig. 3 Comparision between the dimensionless temperature for present work and the results of Matin & Khan [21] for $n$=1, $RR$=2.6, $Ra$=4.7 $10^4$ and $Pr$=0.706.

## 5. Results and discussions

### 5.1 Discussing the isotherms and velocity vectors

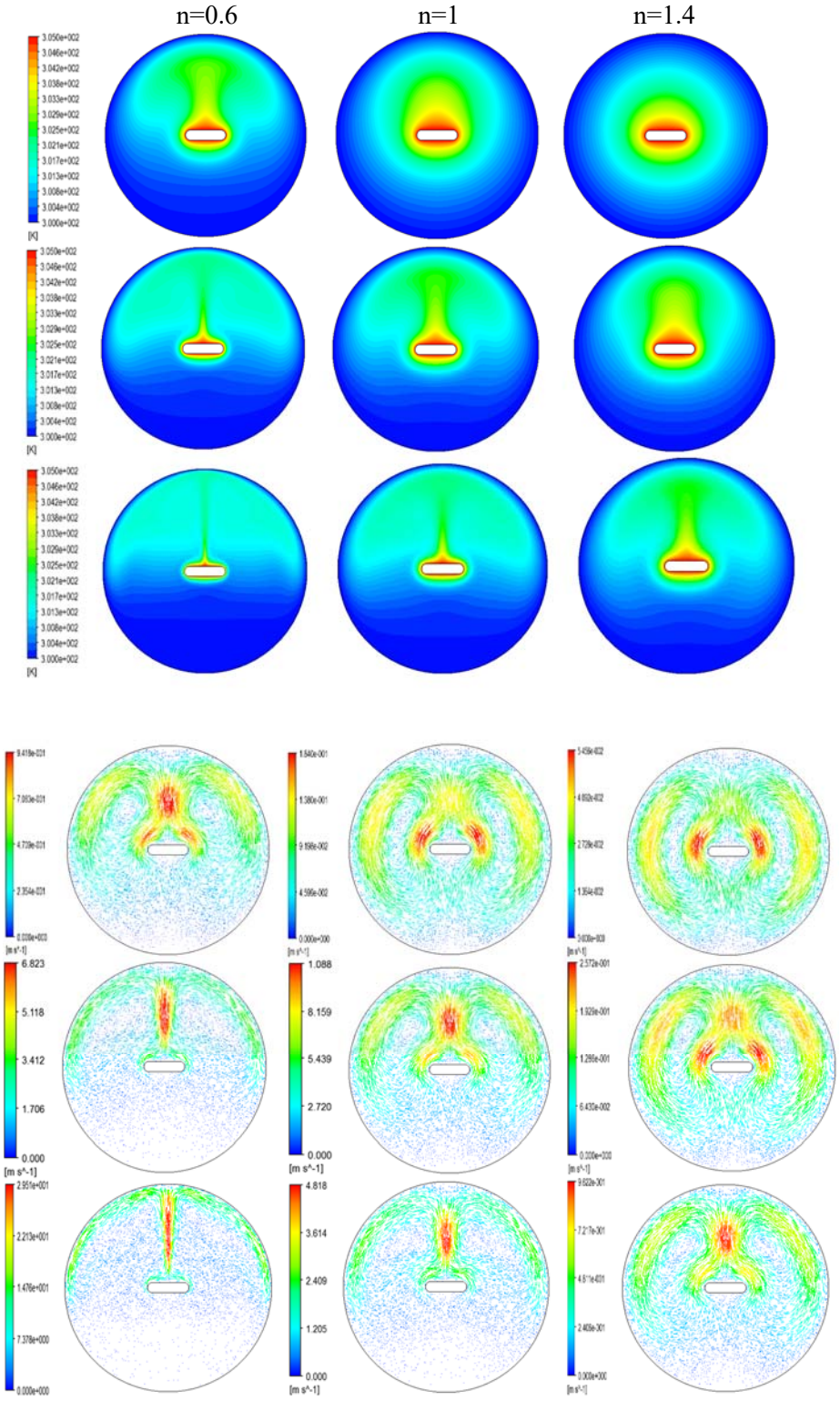


Fig. 4 Isotherms (up) and velocity vectors (down) at Pr=100 for various values of n and Ra; ($Ra=10^3$) first row, ($Ra=10^4$) second row, ($Ra=10^5$) third row.

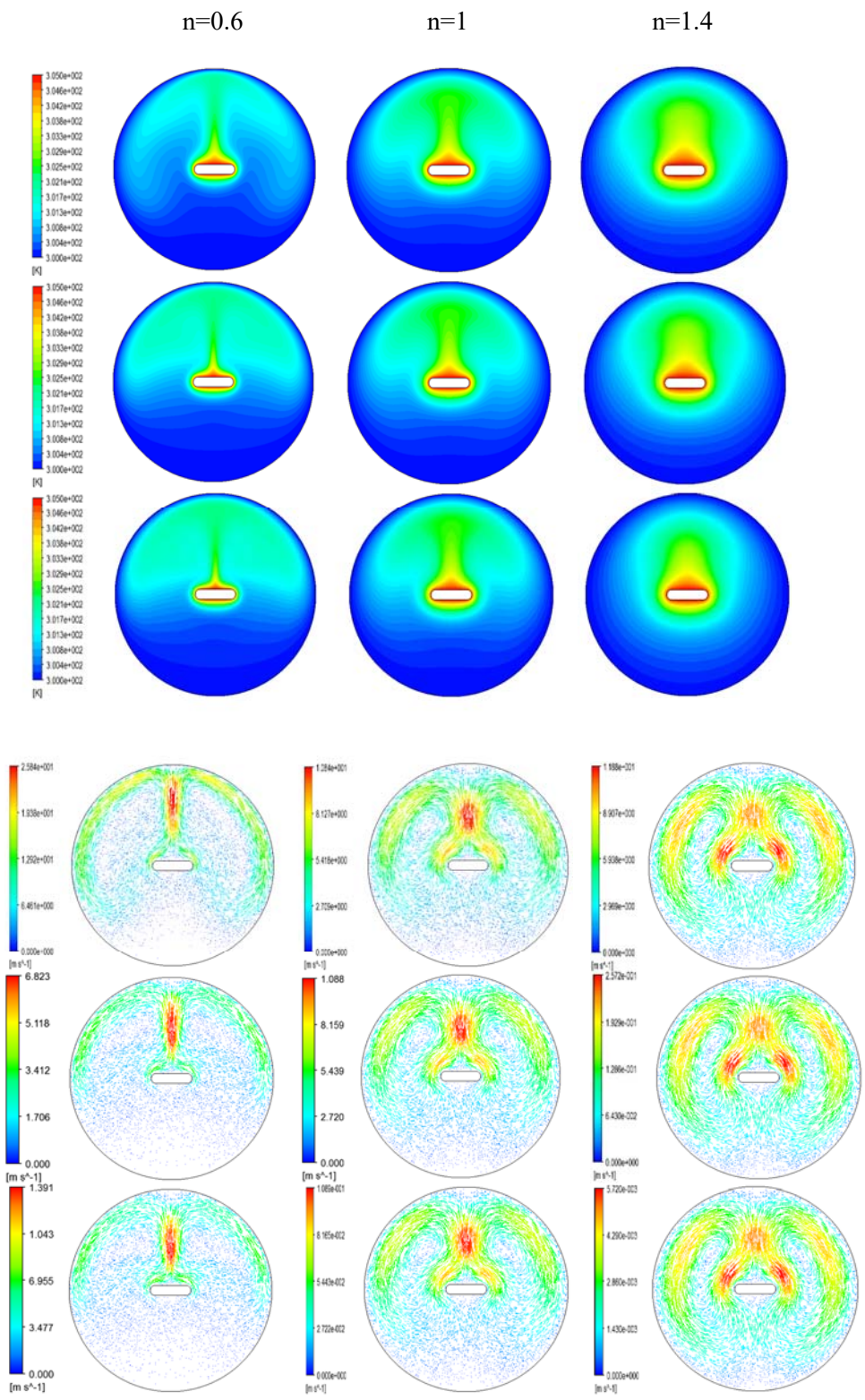


Fig. 5 Isotherms (up) and velocity vectors (down) at $Ra=10^4$ for various values of n and Pr; (Pr=10) first row, (Pr=100) second row, ($Pr=10^3$) third row.

Fig. 4 represents the isotherms and velocity vectors for different power-law indices and Rayleigh numbers at specified Prandtl number. From the figure, It is evident that when we move from shear thinning to shear thickening behavior there is a reduction in the density of isotherms in the vicinity of the heated flat tube and this is due to the increasing in thermal gradient which itself causes the heat transfer rate to increase for pseudoplastic fluids. Furthermore, it is clear that the hot fluid (thermal plume area) is stacked around the flat tube for low values of Rayleigh number ($Ra<10^4$) which is a sign for the small buoyancy force here, the flow movement is almost nonsexist which corresponds with the very weak velocity in this case; Hence, the heat transfer regime in this case is purely by conduction. Then we can see that the increasing in Rayleigh number causes the thermal plume to stretch on top of the flat tube and the cold fluid accumulates at the bottom, the extent of this stretching is a sign for strengthening the buoyancy force, the natural convection takes place within the power law fluid which allows the hot fluid to rise from the flat tube to the upper part of the outer cylinder due to the buoyancy, this can be confirmed from the importance of velocity magnitude for higher Rayleigh number values which indicates that the fluid movement in the gap is rapid.

The effect of the Prandtl number on the temperature and velocity contours is presented in Fig. 5. We can see that the Prandtl number doesn't affect the flow map like the Rayleigh number or the flow index does, in other word it doesn't have too much impact on the heat transfer rate, this is due to the fact that for $Pr>>1$ the hydrodynamic boundary layer thickness is greater than the thermal boundary layer thickness and therefore changing the Prandtl number marginally affects the heat transfer in the thermal boundary layer.

## 5.2 Discussing the dimensionless temperature and velocity

The effects of Rayleigh and Prandtl numbers on the dimensionless temperature are represented in Fig. 6. From the figure, one can see that the power law index n largely affects the dimensionless temperature in the gap by making the thermal plume layer bigger and sharper (the thermal plume region is well seen and well-drawn as n decreases). Also, the power law index n affects the dimensionless temperature in the gap, one can see that when n increases the temperature profiles become more linear (flattened) especially at low Rayleigh number ($Ra=10^3$) and this can help explaining that the mechanism of heat transfer is by conduction more than convection (the dominant heat transfer mechanism is conduction) and the convection effects become very weak in comparison to viscous forces for shear thickening fluids. Finally, one can see that an increase in the Rayleigh number causes a decrease in the dimensionless temperature (especially for shear thinning fluids) and this means that the buoyancy is large.

Fig. 7 reports the variation of the dimensionless velocity as a function of the different parameters. Notice that the increase in the velocity component is correlative related to the increase in the Rayleigh number when the flow index n rest constant. The Rayleigh number effects are clearly seen with the decrease in the flow index n which is a point that the buoyancy force becomes stronger in comparison to the viscous resistance of the flow for decreasing values of n and this effect is particularly prevalent for fluids with $n<1$ due to fluidization.

On the other hand, the effects of convection become increasingly weak compared to viscous forces with an increase in n for shear thickening or dilatant fluids. These effects can be observed in small values of $\bar{\upsilon}$ for $n>1$.

For the Prandtl number, its effects are on hydrodynamic boundary layer more than the thermal boundary layer, these effects on the dimensionless velocity are almost negligible unless for higher values of Rayleigh number ($Ra>10^5$) when the thermal plume region is considerable in the gap, this last one is the biggest for pseudoplastic fluids than the others and for smaller values of prandtl numbers ($Pr<100$) the viscous and thermal diffusion forces cannot be extremely influenced; Thus, the fluid movement is slow.

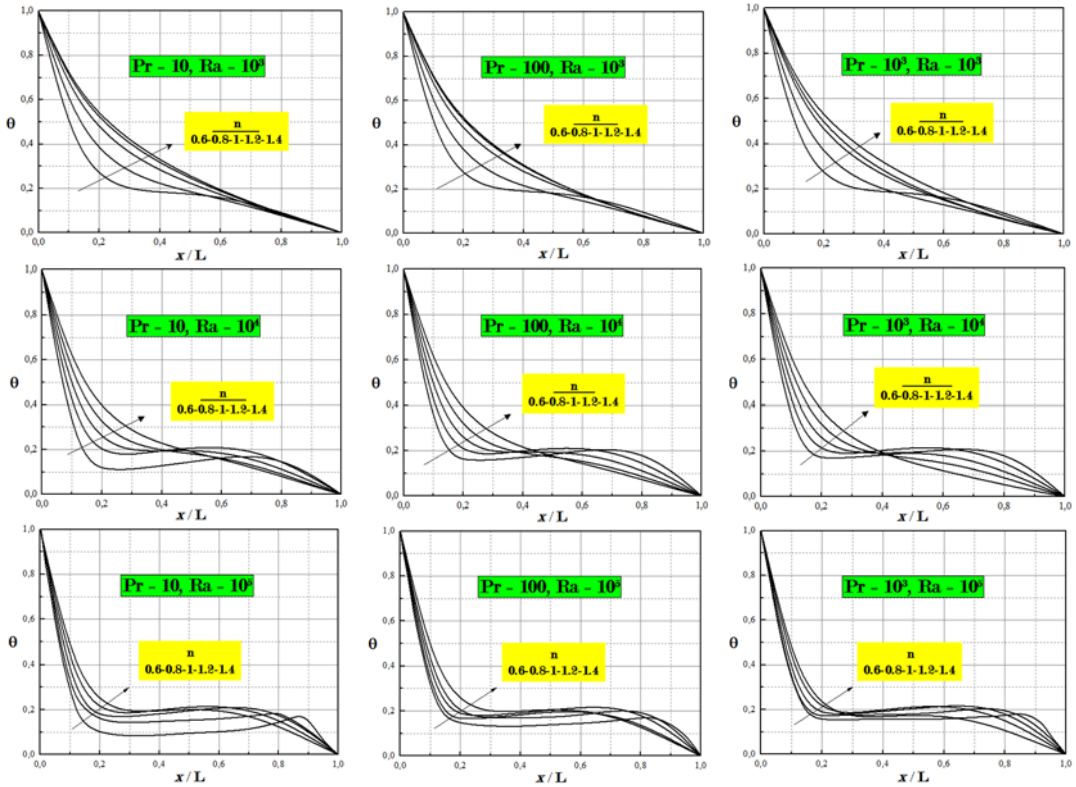


Fig. 6 Dimensionless temperature profiles along the radial line in the gap at ϕ=90° for various parameters of Ra, Pr and n.

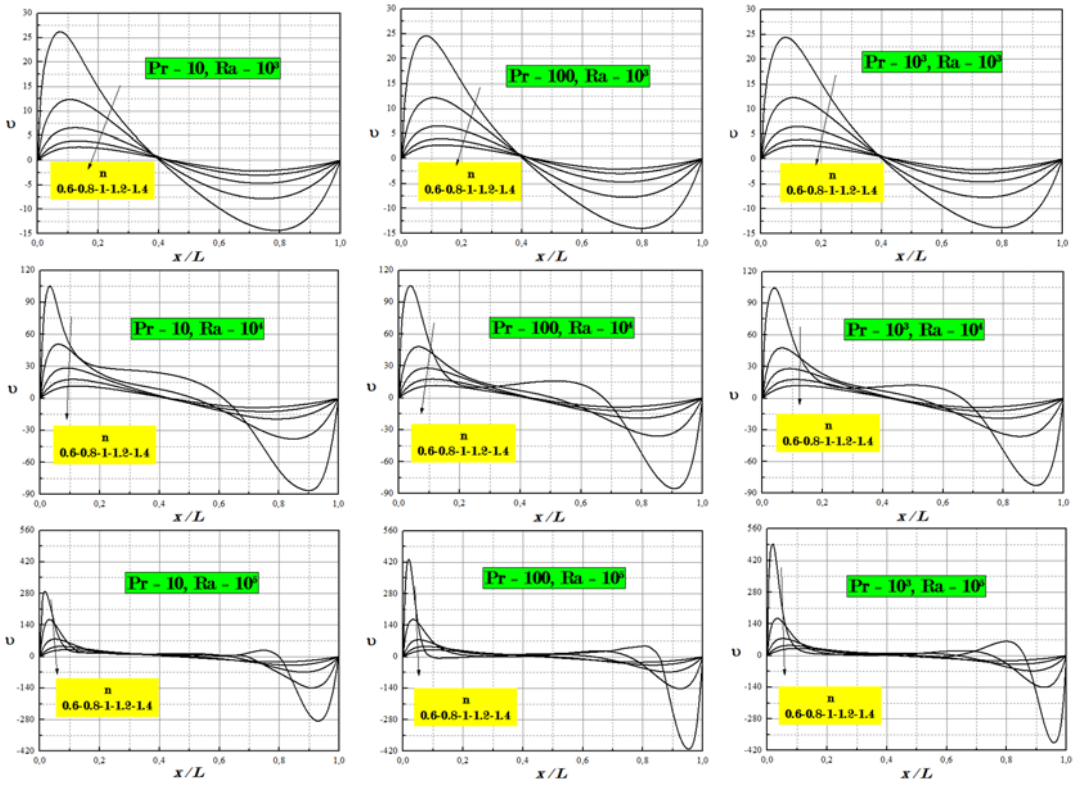


Fig. 7 Dimensionless velocity Profiles along the radial line in the gap at ϕ=90° for various parameters of Ra, Pr and n.

### 5.3 Discussing the variation of the average Nusselt number

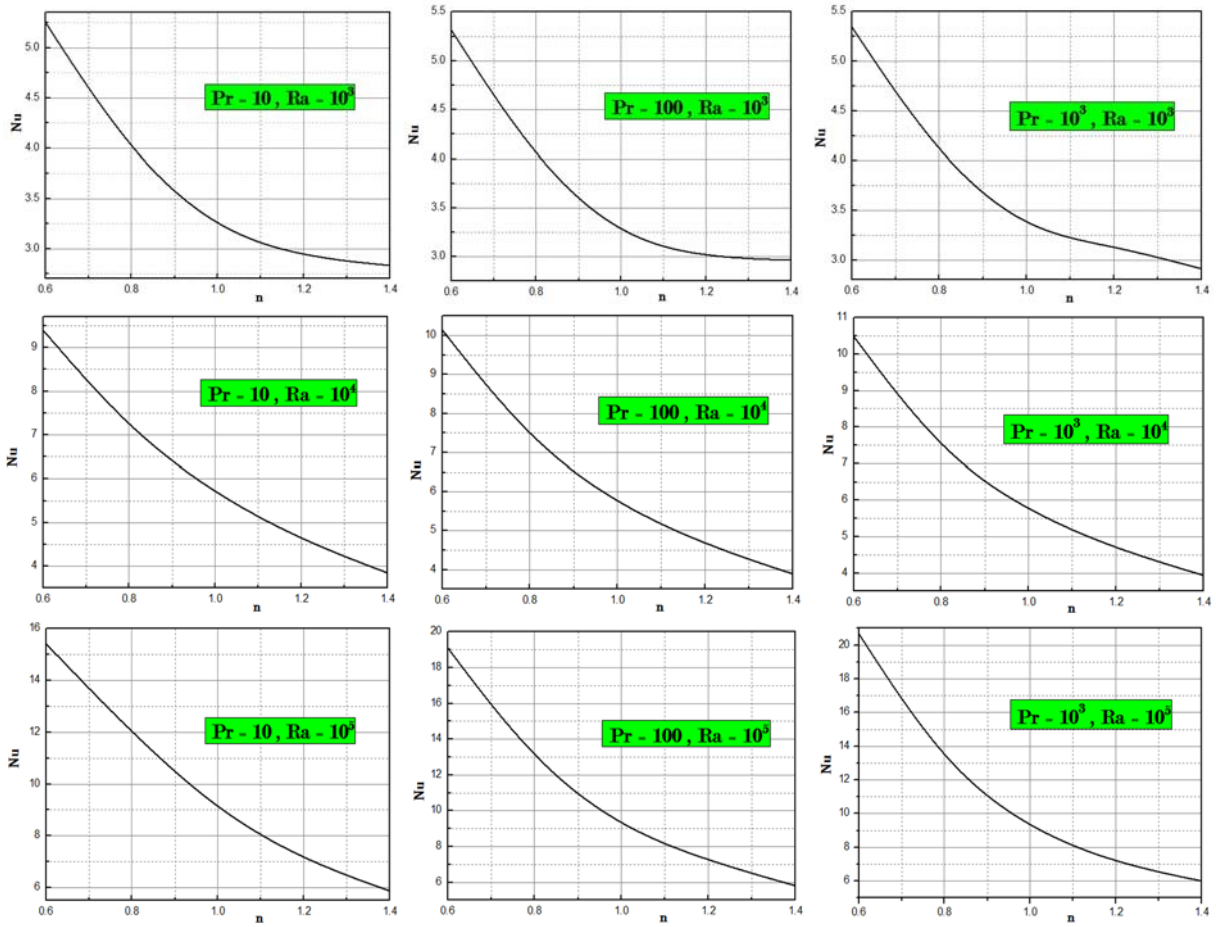


Fig. 8 Variations of the average Nusselt number with the power lawi n for various parameters of Ra and Pr numbers.

Fig. 8 illustrates the variation of the average Nusselt number as a function of the different set of parameters Power law index n, Rayleigh and Prandtl numbers. The figures point out to a reduction in the Nusselt number as the power law augments and this is an indication to the heat transfer enhancement for pseudoplastic fluids (the convection transport in theses fluids is very strong than the others), this is because the effect of shear thickening increases the shear stress between neighboring layers of the fluid and subsequently, minimizing the deformation rate between them which is consistent with the scaling analysis of the viscosity given in equation 7. Notice that this effect is like when the conduction is the dominant heat transfer mode. We deduce that using pseudoplastic fluids can be economical for the efficiency of the heat transfer enhancement.

Furthermore, the Rayleigh number has a determinism impact on the buoyancy force in the gap, it is obvious that the Nusselt number goes higher for increasing values of Rayleigh number, this can be explained by the reality of convection strengthens/weakens with an increase/a decrease in Rayleigh number and that's consistent with the high measures of temperature θ and velocity gradients $\bar{v}$ in Figs 6 and 7, notice that for small Rayleigh number values ($Ra<10^4$) the convection transport is very slow that the conduction is the dominant mode of heat transfer.

On the other hand, Prandtl number varies the relative balance between buoyancy and

viscous forces and doesn't have any influences on the thermal transport in the thermal boundary layer; Therefore, it doesn't seem to have any effects on the variation of the Nusselt number except at high values of Rayleigh number put together with small power law indices, for this case the thermal boundary layer is thinner than the hydrodynamic boundary layer and variation of Prandtl alters the thermal boundary layer thickness which explains the increasing in Nusselt number in this case.

Table 2 concludes everything in this study. As expected, the main parameter which drives the natural convection is the Rayleigh number, a slightly marginal effects of the Prandtl number on the heat transfer, the best case for heat transfer enhancement is that of pseudoplastic fluids where it was found an enhancement of 130 ٪ than Newtonian fluids and diminishment for those of dilatant fluids by about 39 ٪ than the Newtonians. This is fairly complies with the values of Nusselt number in Fig 8.

Table 2 Comparison between the average Nusselt number for the different fluids and different values.

| | $Ra=10^3$ | | | $Ra=10^4$ | | | $Ra=10^5$ | | |
|---|---|---|---|---|---|---|---|---|---|
| | Pr=10 | Pr=100 | $Pr=10^3$ | Pr=10 | Pr=100 | $Pr=10^3$ | Pr=10 | Pr=100 | $Pr=10^3$ |
| $\frac{Nu\,(0.6)}{Nu\,(1)}$ | 1.65 | 1.66 | 1.62 | 1.66 | 1.78 | 1.84 | 1.75 | 2.15 | 2.3 |
| $\frac{Nu\,(1.4)}{Nu\,(1)}$ | 0.89 | 0.92 | 0.88 | 0.68 | 0.68 | 0.69 | 0.63 | 0.61 | 0.62 |

## 6. Conclusion

In the above study, the effect of aiding buoyancy on natural convection from a heated horizontal inner flat tube to its outer cylinder has been studied numerically. The outcomes of the flow and heat transfer characteristics in the gap are presented as temperature and velocity contours, dimensionless temperature and velocity and average Nusselt number. We may deduce the following:

1. The Rayleigh number is largely affects the heat transfer in the gap, it was found that the Nusselt number is proportionable with the Rayleigh number and this attributed to the fact of the Rayleigh number drives the buoyancy strength in the gap and when it's very small ($Ra<10^4$) that cannot creates enough buoyancy the heat transfer is tiny.

2. The Nussselt number is affected by the power law index n and is disproportionable with it, when we decrease n the Nusselt number rises and this means that the heat transfer for pseudoplastic fluids is bigger than that of Newtonian and dilatant fluids. In the best case, there was found an enhancement of about 138 ٪ in the heat transfer rate for pseudoplastic fluids and a reduction of about 40 ٪ for dilatant fluids.

3. The Prandtl number marginally affects the Nusselt number, that's because its effects are on the hydrodynamic boundary layer thicknesses more than the thermal plume layers so one might deduce that the Nusselt number is independent of the Prandtl number.

## References

[1] F. Selimefendigil, H. F. Öztop, A. J. Chamkha, MHD mixed convection and entropy generation of nanofluid filled lid driven cavity under the influence of inclined magnetic fields imposed to its upper and lower diagonal triangular domains, J. Magnetism & Magnetic Materials 406 (2016) 266-281.

[2] M. A. Ismael, T. Armaghani, A. J. Chamkha, Conjugate Heat Transfer and Entropy Generation in a Cavity Filled with a Nanofluid-Saturated Porous Media and Heated by a Triangular Solid, J. Taiwan Institute Chem Eng 59 (2016) 138-151.

[3] G. Sreedevi, R. Raghavendra Rao, A. J. Chamkha, D. R. V. Prasada Rao, Mixed Convective Heat and Mass Transfer Flow of Nanofluids in Concentric Annulus, Procedia Engineering 127 (2015) 1048-1055.

[4] A.J. Chamkha, M. A. Ismael, Natural Convection in Differentially Heated Partially Porous Layered Cavities Filled with a Nanofluid, Num Heat Transfer, Part A: Applications 65 (2014). 1089-1113.

[5] I. Fersadou, H. Kahalerras, M. El Ganaoui, MHD mixed convection and entropy generation of a nanofluid in a vertical porous channel, Computers & Fluids 121 (2015) 164-179.
[6] A.J. Chamkha, Double-Diffusive Convection in a Porous Enclosure with Cooperating Temperature and Concentration Gradients and Heat Generation or Absorption Effects, Num Heat Transfer, Part A: Applications 41 (1) (2002). 65-87.
[7] A. J. Chamkha, H. Al-Naser, Double-Diffusive Convection in an Inclined Porous Enclosure with Opposing Temperature and Concentration Gradients, Int. J Ther Sci. 40 (2001) 227-244.
[8] M. A. Ismael, I. Pop, A. J. Chamkha, Mixed Convection in a Lid Driven Square Cavity with Partial Slip, Int. J Ther Sci. 82 (2014) 47-61.
[9] J. C. Umavathi, J. P. Kumar, A. J. Chamkha, I. Pop, Mixed Convection in a Vertical Porous Channel, Transport in Porous Media, Springer 61 (3) (2005) 315-335.
[10] A. J. Chamkha, S.H. Hussain, Q.R. Abd-Amer, Mixed Convection Heat Transfer of Air inside a Square Vented Cavity with a Heated Horizontal Square Cylinder, Num Heat Transfer, Part A: Applications 59 (2011) 58-79.
[11] S. Hussain, A.K. Hussein, Numerical investigation of natural convection phenomena in a uniformly heated circular cylinder immersed in square enclosure filled with air at different vertical locations, Int Communications in Heat and Mass Transfer 37 (2010) 1115-1126.
[12] A.K. Hussein, Computational analysis of natural convection in a parallelogrammic cavity with a hot concentric circular cylinder moving at different vertical locations, Int Communications in Heat and Mass Transfer 46 (2013) 126-133.
[13] S. Saha, A.K. Hussein, W. Khan, H. Mohammed, W. Pakdee, A. Hasanpour, Effects of diameter ratio of adiabatic circular cylinder and tilt angle on natural convection from a square open tilted cavity , Heat Transfer-Asian Research 41 (2012) 388-401.
[14] Z. Li, A.K. Hussein, O. Younis, M. Afrand, S. Feng, Natural convection and entropy generation of a nanofluid around a circular baffle inside an inclined square cavity under thermal radiation and magnetic field effects, Int Communications in Heat and Mass Transfer 116 (2020) 104650.
[15] Z. Li, A.K. Hussein, O. Younis, S. Rostami, W. He, Effect of alumina nano-powder on the natural convection of water under the influence of a magnetic field in a cavity and optimization using RMS : Using empirical correlations for the thermal conductivity and a sensitivity analysis, Int Communications in Heat and Mass Transfer 112 (2020) 104497.
[16] R.Y. Sakr, Nabil S. Berbish, Ali A. Abd-Aziz, Abdalla Said Hanafi, Experimental and numerical investigation of natural convection heat transfer in horizontal elliptic annuli, Int. J. Chem. React. Eng. 6 (1) (2008) 1-29.
[17] O. A. Alawi, N.A. Che Sidik, H.K. Dawood, Natural convection heat transfer in horizontal concentric annulus between outer cylinder and inner flat tube using nanofluid , International Communication in Heat and Mass Transfer 57 (2014) 65-71.
[18] A. T. Srinivas, R. P. Bharti, R. P. Chhabra, Mixed convection heat transfer from a cylinder in power-law fluids: effect of aiding buoyancy, Ind. Eng. Chem. Res. 48 (21) (2009) 9735–9754.
[19] M. Ohta, M. Akiyoshi, E. Obata, A numerical study on natural convective heat transfer of pseudo-plastic fluids in a square cavity, Num Heat Transfer, Part A: Applications 41, (2010) 357-372.
[20] A. Prhashanna, R. P. Chhabra, Free convection in power-law fluids from a heated sphere, Chemical Engineering Science 65 (1) (2010) 6190-6205.
[21] M.H. Matin, W.A. Khan, Laminar Natural Convection of Non-Newtonian Power-Law Fluids between Concentric Circular Cylinders, Int Commun in Heat Mass Transfer 43 (2013) 112-121.
[22] S. Hussain, A.K. Hussein, R. Mohammed, Studying the effects of a longitudinal magnetic field and discrete isoflux heat source size on natural convection inside a tilted sinusoidal corrugated enclosure, Computers and Mathematics with Applications 64 (2012) 476-488.
[23] A.K. Hussein, S. Hussain, S. Saha, G. Saha, M. Hasanuzzaman, Effects of a longitudinal magnetic field and discrete isoflux heat source size on natural convection inside a tilted sinusoidal corrugated enclosure, J. Basic and Applied Scientific Research 3 (2013) 402-415.
[24] M. J. Uddin, A.K.M. Fazlul Hoque, M.M. Rahman, K. Vajravelu, Numerical simulation of convective heat transport within the nanofluid filled vertical tube of plain and uneven side walls, Int J. Thermofluid Science and Technology 6 (2019) 1-24.
[25] A. Babaie, M. H. Saidi, A. Sadeghi, Electroosmotic flow of power-law fluids with temperature-dependent properties, J. Non-Newtonian Fluid Mechanics 185-186 (2012)

49-57.

[26] O. Turan, A. Sachdeva, N. Chakraborty, R.J. Poole Laminar Natural Convection of Power-Law Fluids in a Square Enclosure with Differentially Heated Side Walls Subjected to Constant Temperatures, J. Non-Newtonian Fluid Mech 166 (2011) 1049-1063.

[27] Z. Alloui, N. Ben Khelifa, H. Beji, P. Vasseur, A. Guizani, The onset of convection of power-law fluids in a shallow cavity heated from below by a constant heat flux, J. Non-Newtonian Fluid Mechanics 196 (2013) 70-82.

[28] M. Lamsaadi, M. Naïmi, M. Hasnaoui, Natural convection of non-Newtonian power law fluids in a shallow horizontal rectangular cavity uniformly heated from below, Heat & Mass Transfer 41 (2004) 239-249.

[29] O. Turan, F. Fotso-Choupe, J. Lai, R. J. Poole, N. Chakraborty, Boundary condition effects on laminar natural convection of power-law fluids in a square enclosure heated from below with differentially heated horizontal walls, Industrial & Engineeing Chemistry Research 53 (1) (2013) 456-473.

[30] O. Turan, J. Lai, R. J. Poole, N. Chakraborty, Laminar natural convection of power-law fluids in a square enclosure submitted from below to a uniform heat flux density, J. Non-Newtonian Fluid Mechanics 199 (2013) 80-95.

[31] A Bejan, Convection Heat Transfer, John Wiley Sons Inc, NY, USA, 1984.

[32] M. Lamsaadi, M. Naïmi, M. Hasnaoui, Natural convection heat transfer in shallow horizontal rectangular enclosures uniformly heated from the side and filled with non-Newtonian power law fluids, Energy Conversion and Management 47 (2006) 2535-2551.

[33] A.K. Hussein, L. Kolsi, R. Chand, S. Sivasankaran, R. Nikbakhti, D. Li, M. Borjini, H. Ben Aïssia, Three-dimensional unsteady natural convection and entropy generation in an inclined cubical trapezoidal cavity with an isothermal bottom wall, Alexandria Engineering Journal 55 (2016) 741-755.

[34] A. Alnaqi, A.K. Hussein, L. Kolsi, A. Al-Rashed, D. Li, H. Ali, Computational study of natural convection and entropy generation in 3-D cavity with active lateral walls, Thermal Science 24 (2020) 2089-2100.

[35] S. Gourari, F. Mebarek-Oudina, A.K. Hussein, L. Kolsi, W. Hassen, O. Younis, Numerical study of natural convection between two coaxial inclined cylinders, Int Journal of Heat and Technology 37 (2019) 779-786.

[36] M. Elkhazen, W. Hassen, R. Gannoun, A.K. Hussein, M. Borjini, Numerical study of electro convection in a dielectric layer between two cofocal elliptical cylinders subjected to unipolar injection, J. Engineering Physics and Thermophysics 92 (2019) 1318-1329.

[37] M. Shirazi, A. Shateri, M. Bayareh, Numerical investigation of mixed convection heat transfer of a nanofluid in a circular enclosure with a rotating inner cylinder, J. Thermal Analysis and Calorimetry 133 (2018) 1061-1073.

[38] M. Sepyani, A. Shateri, M. Bayareh, Investigating the mixed convection heat transfer of a nanofluid in a square chamber with a rotating blade, J. Thermal Analysis and Calorimetry 135 (2019) 609-623.

[39] M. Bayareh, M.A. Kianfar, A. Kasaeipoor, Mixed Convection Heat Transfer of Water-Alumina Nanofluid in an Inclined and Baffled C-Shaped Enclosure, J. Heat and Mass Transfer Research 5 (2018) 129-138.

[40] S.B. Cherif, I. Rahmoune, S. Bougoul, A.J. Chamkha, Analysis of Mixed Convection and Free Convection in a Reduced Solar Collector Using a Nanofluid as Heat Transfer Fluid, Journal of Nanofluids 12 (2023) 877-888.

[41] A.K. Hussein, S. Rout, F. Fathinia, R. Chand, H. Mohammed, Natural convection in a triangular top wall enclosure with a solid strip, J. Engineering Science and Technology 10 (2015) 1326-1341.

[42] A.K. Hussein, H. Ashorynejad, S. Sivasankaran, L. Kolsi, M. Shikholeslami, I. Adegun, Modeling of MHD natural convection in a square enclosure having an adiabatic square shaped body using Lattice Boltzmann Method, Alexandria Engineering Journal 55 (2016) 203-214.

[43] T. Islam, N.Parveen, Md. Fayz-Al-Asad, Hydromagnetic Natural Convection Heat Transfer of Copper-Water Nanofluid within a Right-Angled Triangular Cavity, Int J. Thermofluid Science and Technology 7 (2020) 1-18.

[44] R. Akhter, M.M. Ali, MHD natural convection in nanofluid filled square cavity with isothermally heated hexagonal block, Int J. Thermofluid Science and Technology 9 (2022) 1-9.

[45] Z. Ghoben, A.K. Hussein, The natural convection inside a 3D triangular cross section cavity filled with nanofluid and included cylinder with different arrangements, Diagnostyka 23 (2022) 1-13.

[46] M.Z. Ashraf, S. Rehman, S. Farid, A.K. Hussein, B. Ali, N. Shah, W. Weera, Insight into significance of bioconvection on MHD tangent hyperbolic nanofluid flow of irregular thickness across a slender elastic surface, Mathematics 10 (2022) 2592- 2608.

[47] A. Baïri, N. Alilat, A. Martín-Garín, K. Adeyeye, J.A. Millán-García, L. Roseiro, Free Convective Heat Transfer in a Closed Gap between Concentric Semi-Hemispheres, Energies 14 (2021) Article ID 7479.

[48] P.K. Kar, U. Chetan, A. Kumar, P.K. Das, R. Lakkaraju, Heat transport enhancement and flow transitions in partitioned thermal convection, Physical Review Fluids 8 (2023) Article ID 043501.

[49] K.M. Kim, S.H. Kim, S.T. Lim, T.J. Kim, D. W. Jerng, H.S. Ahn, Geometrical effect of natural convection in an air channel with a cavity at the turning section on thermal behavior and heat removal performance, 203 (2023) Article ID 123792.

[50] C. Dong, S. Chen, W. Tian, S. Qiu, G.H. Su, Numerical Simulation of Natural Convection around the Dome in the Passive Containment Air-Cooling System, Nuclear Engineering and Technology 55 (2023) 2997-3009.

[51] Ansys Fluent User's Guide, Release 6.2.16, Fluent Incorporated, 2013.